



Article

Characterization of Cassava Starch and Its Structural Changes Resulting of Thermal Stress by Functionally-Enhanced Derivative Spectroscopy (FEDS)

Viviana Garces ¹, Angélica García-Quintero ^{1,2} , Tulio A. Lerma ^{1,2}, Manuel Palencia ^{1,*} , Enrique M. Combatt ³ and Álvaro A. Arrieta ⁴

¹ GI-CAT, Department of Chemistry, Faculty of Exact and Natural Sciences, Universidad del Valle, Cali 760032, Colombia; viviana.garces@correounivalle.edu.co (V.G.); angelica.garcia.quintero@correounivalle.edu.co (A.G.-Q.); t.lerma@mindtech.com.co (T.A.L.)

² Mindtech Research Group (Mindtech-RG), Mindtech s.a.s., Barranquilla 080006, Colombia

³ Department of Agricultural Engineering and Rural Development, Faculty of Agricultural Sciences, Universidad de Córdoba, Montería 230002, Colombia; ecombatt@fca.edu.co

⁴ Department of Biology and Chemistry, Faculty of Education and Science, Universidad de Sucre, Sincelejo 700001, Colombia; alvaro.arrieta@unisucra.edu.co

* Correspondence: manuel.palencia@correounivalle.edu.co



Citation: Garces, V.; García-Quintero, A.; Lerma, T.A.; Palencia, M.; Combatt, E.M.; Arrieta, Á.A. Characterization of Cassava Starch and Its Structural Changes Resulting of Thermal Stress by Functionally-Enhanced Derivative Spectroscopy (FEDS). *Polysaccharides* **2021**, *2*, 866–877. <https://doi.org/10.3390/polysaccharides2040052>

Academic Editor: Rajkumar Patel

Received: 5 September 2021

Accepted: 22 October 2021

Published: 3 November 2021

Publisher's Note: MDPI stays neutral with regard to jurisdictional claims in published maps and institutional affiliations.



Copyright: © 2021 by the authors. Licensee MDPI, Basel, Switzerland. This article is an open access article distributed under the terms and conditions of the Creative Commons Attribution (CC BY) license (<https://creativecommons.org/licenses/by/4.0/>).

Abstract: Starch is one of the biopolymers that has been recognized as promising for its application as an eco-friendly substitute for conventional polymers due to its biodegradable nature, low cost, and considerable abundance from renewable vegetal-type resources. In particular, the use of cassava starch as raw material in the manufacture of packaging materials has increased in recent years. Consequently, the analytical study of the quality and features of starch and its derivatives throughout their entire life cycle have gained importance, with non-destructive sample methods being of particular interest. Among these, spectroscopic methods stand out. The aim of this study was evaluated using spectroscopic techniques (i.e., mid-infrared spectroscopy (MIRS) and functional-enhanced derivative spectroscopy (FEDS)) for the monitoring of the effect of the thermal stress of starch in conjunction with computational tools such as density-functional theory (DFT). It is concluded that the FEDS technique in conjunction with DFT calculations can be a useful tool for the high-precision spectral analysis of polymers subjected to small thermal perturbations. In addition, it is demonstrated that small changes produced by thermal stress can be monitored by infrared spectroscopy in conjunction with FEDS at wavenumber range between 3800 and 3000 cm^{-1} , which would allow for the implementation of spectral techniques instead of thermal techniques for out-lab evaluations and for the study of the thermal stress of biomaterials.

Keywords: cassava starch; mid-infrared spectroscopy; functional transformations; derivative spectroscopy; thermal stress

1. Introduction

Polymers derived from natural sources are widely recognized as one of the most environmentally friendly and appropriate alternatives to replace fossil-fuel based polymeric materials [1,2]. Thus, biodegradable polymers based on low molecular weight biomolecules such as sorbitol, dextrose, and citric acid (as well as in natural macromolecules such as agar, cellulose, collagen, lignin derivatives, cellulosic biomass, and starch) have been widely studied for their use in multiple applications including both structural and functional applications [3–9]. Starch is one of the biopolymers that has been recognized as promising for its application as an eco-friendly substitute for conventional polymers due to its biodegradable nature, low cost, and considerable abundance from renewable vegetal-type resources. Thus, starch has been used as a raw material for biofuel production, in the food industry as a thickener and stabilizing agent, as an encapsulation material for bioactive

substances, in the generation of starch-based conductive polymers, and in the production of biodegradable polymeric packaging, among others interesting applications [3,8,10–15].

Starch is a polysaccharide formed by a mixture of high molecular weight polyols denominated amylose and amylopectin [14,16,17]. The proportion between both polysaccharides in starch depends on the type of plant material from which they are extracted (i.e., corn, potato, wheat). The cassava tuber (*Manihot esculenta*) is one of the most relevant sources in tropical and subtropical regions, whose dry weight is approximately 84% of amylose and amylopectin [13,18,19]. In structural terms, both homopolymers are composed of fundamental monomeric glucose units in their hemiacetal form α -D-glucopyranose [19]. In the case of amylose, it is a linear biopolymer made up of α -(1 \rightarrow 4) glycosidic type bonds between approximately 500 to 2000 units. As for amylopectin, this is a branched type homopolysaccharide made up of up to 1000 units with the presence of α -(1 \rightarrow 4) glycosidic bonds with α -(1 \rightarrow 6) glycosidic type branches, which constitute approximately between the 6 to 5% of the structure [15,19–23]. Chemical and structural composition of starch makes it a polymer with high hydrophilicity, high susceptibility to humid conditions, limited processability, reduced solubility in water, instability against temperature changes, and low resistance to shear. For these reasons, its mechanical and functional properties limit its widespread use in the polymer industry, particularly in the development of packaging-type systems [3,4,7,19,22].

Generally, thermal stress has been used as an economical and environmentally friendly treatment method for biopolymers (e.g., wood, starch, proteins) and produces changes in its functional and mechanical properties (e.g., glass transition temperature, durability, heat capacity, etc.). These changes are mainly caused by variations in the water contents in the biopolymer matrix that lead to structural and conformational changes of its native structure by modifying the molecular mobility of the systems [24–26]. In this work, it is crucial to monitor the functional and mechanical characteristics of the starch, derivatives, and starch-based polymer mixtures without carrying out the destruction of the samples (this being a very common situation in the study of the thermal stress of biopolymers). Usually, the effect of temperature on starch has been studied through differential scanning calorimetry to study the variation of its properties during their production and processing (e.g., to estimate the heat transported through the aqueous medium during gelatinization [4,27], or to study the effect of heat stress on the physicochemical properties of starch [28]), studies which have been commonly focused on starch from maize. In particular, thermal stress during the heating of food, sterilization operations, or inadequate storage conditions can alter the barrier properties of starch-based materials and affect their functionalities [5,14,22,28–30]. Therefore, in recent years there has been increased interest in both the use of cassava starch as a raw material in packaging manufacturing as well as the use of spectroscopic techniques (e.g., mid-infrared spectroscopy (MIRS) and functionally-enhanced derivative spectroscopy (FEDS)) for monitoring the effect of their thermal properties. In conjunction with computational tools such as the functional density theory (DFT), the study of changes in the structural properties of starch-based materials has been explored.

In particular, MIRS is of special interest since the analytical information it has provided is associated with the fundamental vibrations of functional groups, allowing for their identification, the analysis of their molecular interactions, and their straightforward quantification using a calibration curve. In addition, this allows one to omit the use of multivariate calibration models which are usually characterized to require a large proportion of samples (as in the case of near-infrared spectroscopy) [18,31,32]. However, despite the multiple advantages present in MIRS analysis, in polymeric systems such as starch the structural characterization by MIRS of the signals associated with molecular vibrations presents hidden and overlapped signals, making it difficult to interpret the spectrum correctly and limits the information obtained through this; it is complicated to establish specific vibrational frequencies beyond typical vibration ranges. For example, in the case of the stretching region of the O–H bonds, they present a slight perceptible displacement and a widening associated with the effect of hydrogen bonds. In the region

between 1100 cm^{-1} and 900 cm^{-1} (associated with stretching of C–O, C–H, C–O–H bonds), and bending C–O–H bonds, it is difficult to reliably identify the vibrational modes since they are overlapping and poorly resolved signals [21,31,33,34]. A solution to this situation is to use deconvolution methods to increase the spectral resolution of the signals in the MIRS associated with the vibration frequencies of the molecular system [35]. FEDS is a method based on functional transformations of simple implementation that allows for the deconvolution of the infrared spectrum, enabling the analysis of multiple overlapping and hidden signals [7,36]. This tool has been evaluated with optimal results in the identification of non-appreciable signals in the pristine infrared spectra and in the evaluation of the influence of the molecular interactions on the frequency of vibration in systems of simple molecular composition (e.g., mixtures of controlled composition), as well as in the study of complex systems of biological origin (e.g., animal tissue, bacterial biofilms, soil samples). Likewise, this tool has been used in the analysis of polymeric matrices based on PVC, polyurethanes, polyureas, cellulose, and polymer-clay composites [31,36–42]. Thus, the application of FEDS in the analysis and characterization of biopolymer mixtures, such as cassava starch and its derivatives, is a promising analytical approach for the study of its quality and features throughout their entire life cycle.

2. Materials and Methods

2.1. Source and Thermal Treatment of Cassava

Commercial cassava starch (Almidones 1-A, Cali, Colombia) was used to carry out the experiments. In order to analyze the effect of thermal stress, the cassava starch was subjected to thermal heating, employing an air atmosphere temperature-programmed heating oven at $105\text{ }^{\circ}\text{C}$ for 4 h.

2.2. Analysis by Infrared Spectroscopy with Fourier Transform Coupled to the Total Attenuated Reflectance Technique (FTIR-ATR)

The infrared spectra of the native, thermal product, and acetylated cassava starches were obtained using a Fourier-transform infrared spectrometer coupled to the attenuated total reflectance technique with ZnSe crystal (IR-Affinity, Shimadzu, Kyoto, Japan). The analysis region was $4000\text{--}600\text{ cm}^{-1}$. Fifteen readings were collected and averaged with a resolution of 2 cm^{-1} . All samples were analyzed for triplicate.

2.3. FEDS Analysis

The FEDS treatment of the pristine infrared spectra of cassava starch and its acetylated derivatives was carried out using the methodology described by Palencia (2020) [35]. In general, this process consists of applying a smoothing algorithm to the infrared spectrum data with an average-based spectral filter of the absorbance and the wavenumber with a data window of 3 in 20 cycles. The obtained spectrum is subsequently auto-scaled using the maximum and minimum absorbance values, and the FEDS algorithm is applied to the processed data based on the first derivative of the inverse of auto-scaled spectra, the square root of its absolute value, and the inverse of the resulting data. The conceptual foundation and the specific mathematical procedure of deconvolution are reported in detail in previous scientific articles [35,36,43].

2.4. Computational Analysis

The computational calculations were developed using the Gaussian 09W/Gauss view 5.0.8 software package applying Density-functional theory (DFT) with the B3LYP hybrid functional and the 6-31G + (*d*) basis set, considering the singlet state and neutral charge for the gas phase. This level of theory has been accepted as an appropriate approach to analyze a simplified molecular model of biopolymers such as arabinogalactan and chitosan [44,45]. In this sense, in the present study, the DFT/B3LYP/6-31 G + (*d*) level of theory has been employed as a first approximation to analyze and compare the infrared spectra of model units of amylopectin, amylose, and representative structures of their acetylation products.

3. Results and Discussion

3.1. Cassava Starch Characterization at 25 °C and Starch Dried at 100 °C

Starch spectra at 25 °C and starch dried at 100 °C are shown in Figure 1. The typical assignation of starch includes the wide band associated with hydroxyl groups (O-H stretch among 3600 and 3100 cm^{-1}), typical signals associated with $-\text{CH}$ and $-\text{CH}_2$ units (among 2950 and 2850 cm^{-1}), vibrations of side chain ($\text{CH}_2\text{-OH}$) at 1320 cm^{-1} (3), vibrations C-O and C-C at 1145 cm^{-1} (4) and 1080 cm^{-1} (5), respectively. The signal (4) has been described as being associated with glycosidic bonds [46–49], and an intense signal has been associated with vibrations of C-O-H (bending) at 1000 cm^{-1} (6). This signal is particularly interesting since its correlation with the content of glucose in aqueous dissolutions has been described [49]. However, it is important to indicate that signal pattern among 1700 cm^{-1} and 900 cm^{-1} are consistent with signals described for glucose, which is the monomer unit of amylose and amylopectin (which have been identified with numbers from 1 to 6 in Figure 1) [49]. The signal at 1420 cm^{-1} (2) has been described to be the bending of CH and CH_2 [46,47]. In particular, signal associated to $\sim 1650 \text{ cm}^{-1}$ (1) is usually described as water bending vibration due to highly hydrophilic nature of polymer structure [46–49]. However, it is important to note that signals are present both in the samples at 25 °C (room temperature) and at 100 °C (dried samples in oven). Therefore, it is suggested that, if sample is not disturbed for air humidity, then the hydrophilicity of starch and/or its hydration degree can be easily monitored by using of signal (1).

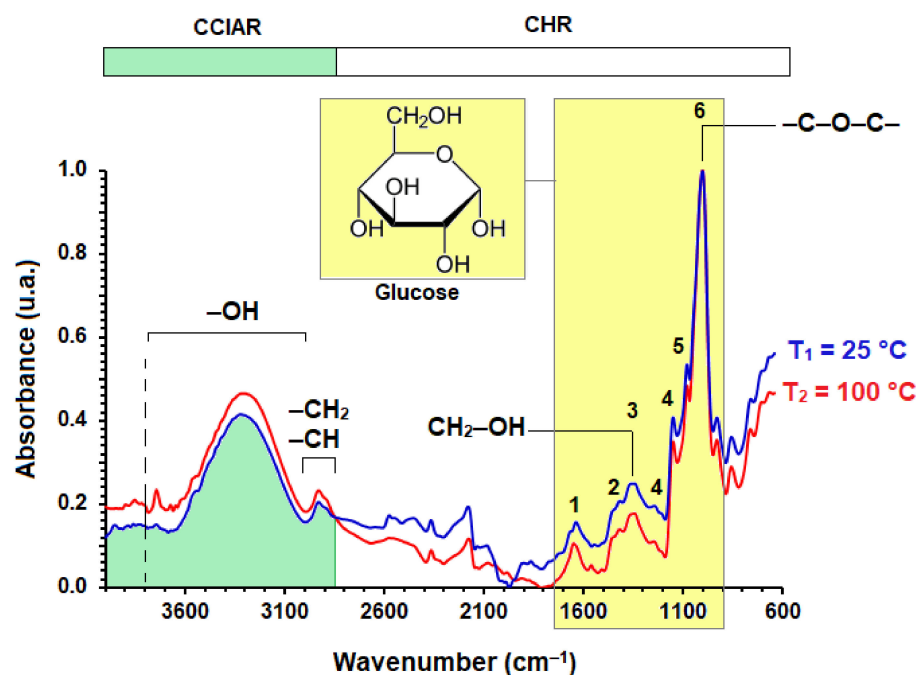


Figure 1. Averaged infrared spectra of starch at 25 °C ($T_1 = 25 \text{ °C}$) and after to be subjected to thermal stress at 100 °C ($T_2 = 100 \text{ °C}$). (CCIAR and CHR mean chain-chain intermolecular association region and chain hydration region, respectively).

When trajectories of line functions of spectra are compared, it can be seen that among 4000 cm^{-1} and $\sim 2850 \text{ cm}^{-1}$ the intensity of absorption for starch dried at 100 °C is larger than absorption intensity observed for starch at 25 °C. However, it is well-known that in this region not only is the contribution of hydroxyl groups present, but a contribution of water molecules absorbed is also expected. Therefore, from a compositional point of view, for “dried” starch, a decreased absorption intensity is expected due to loss of water molecules resulting from heating. However, a decreasing of intensity was not observed in this first wavenumber range. On the other hand, for wavenumbers lower than $\sim 2850 \text{ cm}^{-1}$, a consistent behavior of spectral trajectories respect to the drying operation is obtained (i.e.,

at lower absorbed water content a lower contribution of water spectrum to starch spectrum, and therefore, the absorption intensity of “dried” starch is lower than those observed for starch at room temperature).

The behavior among 4000 cm^{-1} and $\sim 2850\text{ cm}^{-1}$ can be explained for an increase of interchain space as a result of heating. However, the effect of temperature on thermal properties of starch has been described to be more complex than a simple increase of intermolecular space. First, it is recognized that starch is characterized by a multilevel structure from the macro- to the molecular scale [50]. In this way, it is clear that heating influences the amorphous and crystalline domains. However, it also promotes desorption of water molecules (this being an aspect important for the description of gelatinization of starches), which is an irreversible process associated with the alteration of molecular ordering, temperature, heating time, and moisture content, among others aspects [50–52]. In general, the presence of water is associated with the disturbance of the crystalline regions and, consequently, the vibration of polymer chains is favored. However, it is widely accepted that water content has an important effect on melting temperature (T_m). Thus, T_m of starch is increased by reducing of moisture content [50]. From a practical perspective, water can be assumed to act as a plasticizer. In this regard, an increase of specific heat with the increase of temperature and moisture content has been described for Cassava starch. Thus, e.g., a variation in water content in starch from 4% to 30% produces a change in specific heat from 267.6 to 412.2 J/kgK at 25 °C, while at 75 °C the specific heat changes from 368.9 to 545.1 J/kgK for similar water contents [51]. Besides, it has been described that starch thermal conductivity decreases with the temperature and the moisture content, which it has been associated with a decrease of crystalline structure and an increase of amorphous domains [51,52]. Therefore, an important result is identifying two zones. The first is a starch's spectrum zone where thermal stress can be observed, while the second is a region where hydration can be evaluated. In this way, two regimes can be defined: (i) a chain-chain intermolecular association region (CCIAR), which is associated with spectral changes associated with the thermal response of polymer chains by effect of the increase on temperature and decrease of moisture content; and (ii) a chain hydration region (CHR), which is characterized by the interaction of hydrophilic groups with water molecules (see Figure 1).

3.2. Study by FEEDS of Chain-Chain Intermolecular Association Region Associated to the Hydroxyl Band

As previously established, the region between 4000 and $\sim 2850\text{ cm}^{-1}$ can be used to study the effect of thermal stress on the intermolecular ordering characteristics of starch. In order to explore previous affirmation, the spectrum region among 3800 cm^{-1} and 3000 cm^{-1} was selected since this is associated with hydroxyl groups and can be easily contrasted with results obtained by molecular simulation of infrared spectra of molecular models (dimers of amylopectin and amylose).

In Figure 2A,B infrared and FEEDS normalized spectra for starch at 25 °C ($T_1 = 25\text{ °C}$) subjected to thermal stress ($T_2 = 100\text{ °C}$) are shown. According to the FEEDS spectra, a set of signals can be associated with both samples (i.e., C1 which is related with maximum absorbance, and others “unknown” signals which usually are not described in the spectral analysis of the starch, some are around the absorbance maximum and others can be identified among 3800 and 3600 cm^{-1} (note that it is important the performing of replicates to reduce the appearing of artefacts resulting of nature fluctuation of signal, in this way, the use of replicates, smoothing algorithms and correlation analysis of signals were used in order to warrant a correct analysis). To ease the analysis, different features of spectrum were denoted as C1, C2, C3, C4, and C5. Detailed analysis is shown below.

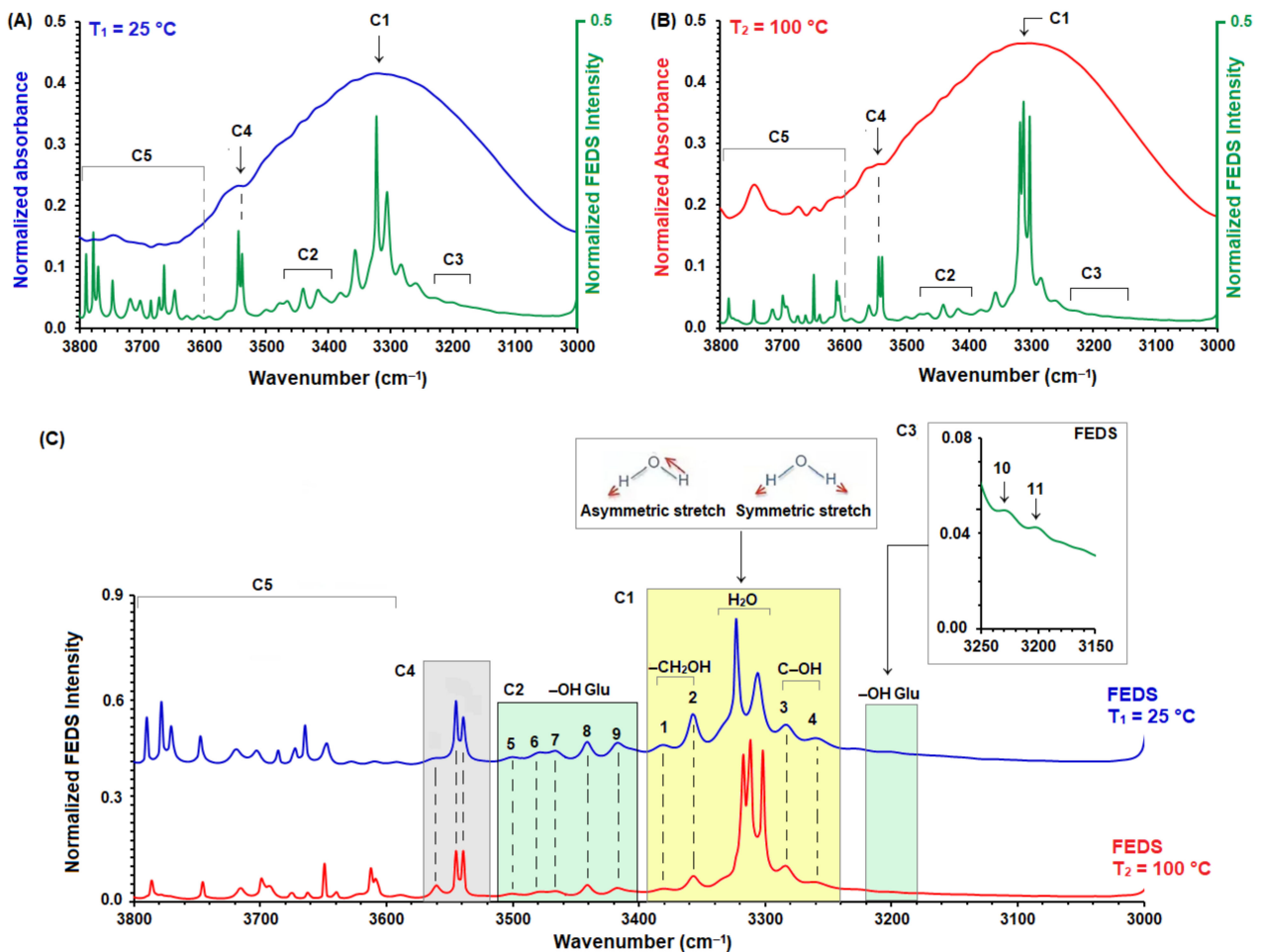


Figure 2. Normalized infrared and FEDS spectra of Cassava starch for T_1 (A) and T_2 (B) among 3800 and 3000 cm^{-1} , and (C) comparison of FEDS spectra for T_1 and T_2 among 3800 and 3000 cm^{-1} .

In region C1, one can identify two sets of signals, namely ones related with the maximum absorbance and others distributed around of center signals. By comparison with the FEDS spectrum of liquid water which was previously published [36], it can be established that FEDS signals in the center of band correspond to asymmetric and symmetric stretching of water.

Therefore, it is verified that absorbed water molecules are usually in the starch due to high hydrophilicity. This result is consistent with previous works [46–49]. By comparison of FEDS spectra, a displacement of water signals can be observed in T_2 compared with T_1 (this displacement can be verified by the use of adjacent signals as referencing points; Note that signals 1, 2, 3, and 4 remain invariant in both spectra). Thus, water signal displacement is a result of thermal stress and can be explained by the destruction of crystalline domains and the subsequent formation of amorphous domains with a larger interchain space. During drying, water is drawn from the surface of the starch, but not completely removed. Furthermore, after subsequent cooling, water molecules are again absorbed from the medium. In this way, the presence of water between the samples is not surprising, however, it is clear from the results that the increase in the intermolecular space of the chains weakens the interactions between them (i.e., hydrogen bonds), and therefore a greater infrared absorption is expected for T_2 with respect to T_1 .

On the other hand, signals 1, 2, 3 and 4 are associated with structural vibrations of the OH groups that form the monomer of starch polysaccharides. The above is supported for the absence of changes in the position of signals compared to previously published spectra. FEDS spectrum of ethanol and methanol is characterized by signals associated

with hydroxyl groups to the left of the water FEDS signals [36]. From the database of ATR-IR spectra and previous publications, signals at $\sim 3392\text{ cm}^{-1}$ (1) and 3193 cm^{-1} (11) can be identified [53]. From computational analysis, signals at $\sim 3502\text{ cm}^{-1}$ (5), 3482 cm^{-1} (6), 3460 cm^{-1} (7), and 3443 cm^{-1} (8) have been previously described [54]. In particular, a signal at 3418 cm^{-1} (9) was related to α -D-anomeric glucose [54]. Thus, the above permits one to associate the signal 9 with a specific structural characteristic the great interest.

On the other hand, signal C4 can be identified in both spectra with an exact correlation. In consequence, these signals are associated with hydroxyl groups of monomer structure. However, signals contained in C5 do not correlate adequately, so their origin is understood from the structural complexity at the intermolecular level producing a consistent complexity of spectrum. In Figure 3, the theoretical spectra of amylose and amylopectin dimers (A and C) and their respective structures (B and D) is shown. It can be observed that signals between 3800 and 3600 cm^{-1} are associated with signals of polysaccharides constituting the starch (i.e., amylose and amylopectin). Signals calculated for dimers are summarized in Table 1.

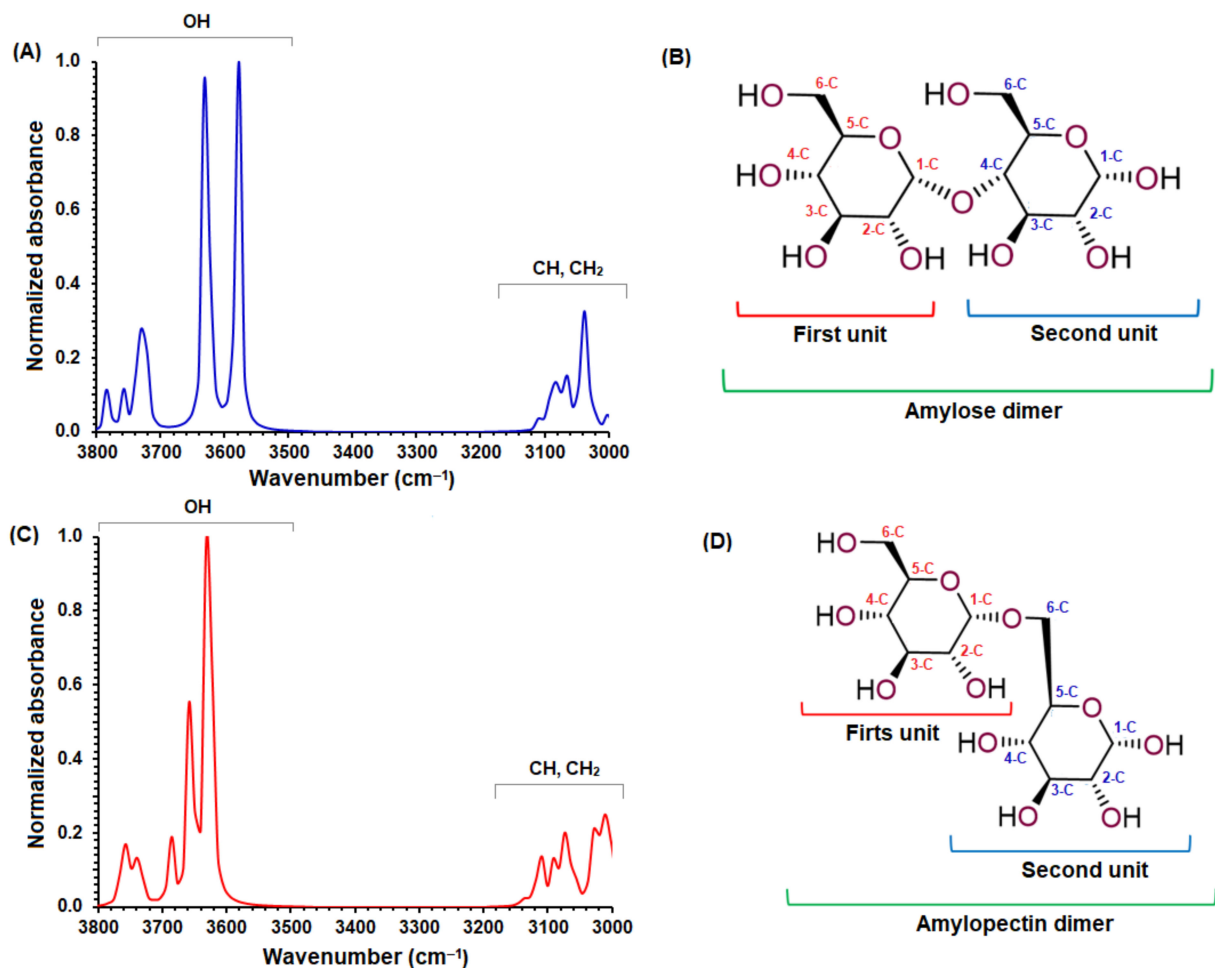


Figure 3. Theoretical spectra of amylose and amylopectin dimers (A,C) and their respective structures (B,D).

Table 1. Signals between 3800 and 3500 cm^{-1} obtained through DFT calculations for dimers of amylose (2Am) and amylopectin (2AmP).

Theoretical Wavenumber (cm^{-1})			Signal Assignment
2Am	2AmP	Total	(From Theoretical Data)
3784		3784	6-C of 2Am-m1
3757	3757	3757	6-C of 2AmP-m1 or 2AmP-m2
	3739	3739	1-C of 2AmP-m2
3730		3730	3-C of 2Am-m2 and 2AmP-m1
	3685	3685	2-C of 2Am-m2
	3658	3658	4-C of 2Am-m2
3631	3631	3631	6-C 2Am-m2 and 2-C 2AmP-m1
3577		3577	2-C of 2Am-m2

"Total" refers to 2Am + 2AmP (sum of individual spectra). All Signals assignment were based on structures B and D in Figure 3. "-m1" and "-m2" refer to "first unit" and "second unit", respectively.

From results of DFT of dimers, it can be seen that signals associated to CH and CH_2 appear among 3120 and 3000 cm^{-1} . However, these signals are expected under to 3000 cm^{-1} . These displacements of $\sim 70 \text{ cm}^{-1}$ are explained due to oversimplifications of molecular models used for the description of system under study. Thus, intermolecular interactions, nature of condensed phase, polymeric nature, and molecular organization of chains are not considered. Consequently, experimental signals of hydroxyl vibrations are expected to show a displacement to the right respect to theoretical results. Here, it was assumed that the behavior is displacement should show a more or less similar magnitude. Hence, from displacement of $-\text{CH}_2$ and CH signals experimentally obtained and calculated by DFT was estimated a displacement constant $k = 184 \text{ cm}^{-1}$ (k was obtained by comparing the average signals of all signals related to $-\text{CH}_2$ and $-\text{CH}$ units in the samples). Nevertheless, assignment of signals by theoretical data must be carried out carefully. Therefore, due to working spectral resolution $\Delta v = 2 \text{ cm}^{-1}$, there is an inherent uncertainty of $\pm 2 \text{ cm}^{-1}$, and since FEDS uses the difference of two consecutive data to obtain a new data set, the tolerance to define when two signals are significantly equal was assumed to be $\pm 4 \text{ cm}^{-1}$. In this way, if the difference among two signals is lower than 4 cm^{-1} then it is concluded that signals are the same. Also, the approximate origin of k implies that a greater tolerance is admissible as long as the assignment shows to be consistent with the data. Thus, by previous criteria, signals obtained by FEDS can be assigned from theoretical calculations (see Table 2).

Table 2. Assignment of signals by FEDS and DFT ($k = \sim 184 \text{ cm}^{-1}$).

$v \text{ (cm}^{-1}\text{)}$ by DFT	$v - k \text{ (cm}^{-1}\text{)}$	$v \text{ (cm}^{-1}\text{)}$ by FEDS	Observations
3784	3600	3609	6-C of 2Am-m1
3757	3573	3590	1-C of Am-m2; 6-C or 3-C of 2AmP-m1 or 2AmP-m2
3739	3555	3561	1-C of 2AmP-m2
3730	3546	3545 3539	Signal splitting in 3-C of 2Am-m2 and 2AmP-m1 (no specific assignment)
3685	3501	3502	2-C of 2Am-m2
3658	3474	3482 3460	Signal splitting in both cases related to 4-C of 2Am-m2 (no specific assignment)
3631	3447	3443 3418	Signal splitting in 6-C of 2Am-m2 and 2-C of 2AmP-m1 (no specific assignment)
3577	3393	3392	2-C of 2Am-m2

DFT, density-functional theory; k , displacement constant; v , wavenumber.

From the analysis shown in Table 2, it can be concluded that these signals are related to the amorphous phases of starch. Furthermore, since the crystalline phases are expected to show a more significant interaction between their components, which is an aspect not considered in the working models, the results obtained by DFT will correspond to systems with a low restriction in their vibrational modes. When a phase is more crystalline, strong intermolecular interactions are associated with the polymer structure due to high molecular ordering. As a consequence, a larger vibrational energy is required since the movement of molecular segments is more restricted. Consequently, vibrations related to crystalline phases are expected to demonstrate larger wavenumbers (i.e., according to our data wavenumbers larger than $\sim 3610\text{ cm}^{-1}$).

By comparing T_1 and T_2 spectra, signals associated with the crystalline phase were assigned (see Figure 4). For this, the correlation of signals resulting from FEDS were identified by direct comparison of spectra. The above was performed in order to identify the signals from the infrared spectrum transferred to the FEDS spectrum (i.e., inherited signals). Later, the signals calculated by DFT were assigned preserving the sequence of appearance in the theoretical spectrum in order to use the relative position of the signals for their identification. From Figure 4, it is concluded that changes into spectra, promoted by thermal stress, are related to the spectrum zone recognized to show vibrations from the crystalline domains. The previous conclusion is consistent with the fact that elimination of water from starch alters the crystalline phases [50–52]. At experimental conditions of this work, by gravimetry, it was established that the loss of water mass was $13 \pm 1\%$. In particular, here it is demonstrated that these small changes can be monitored by infrared spectroscopy in conjunction with FEDS.

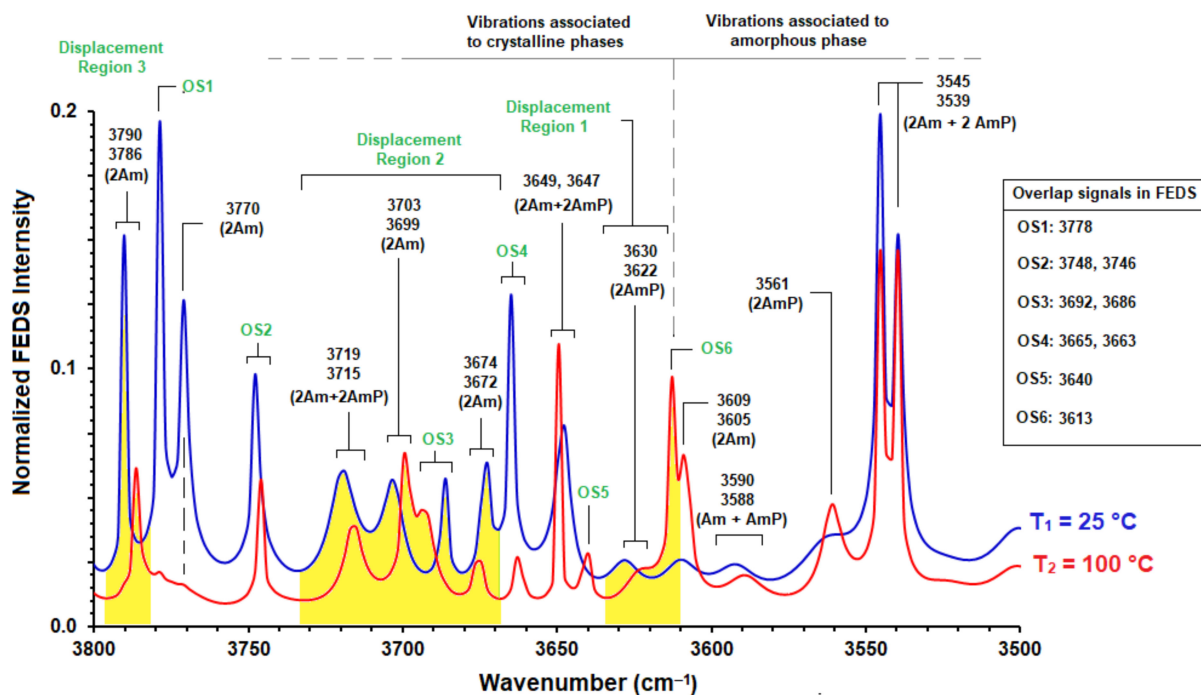


Figure 4. Comparison of spectra T_1 and T_2 between 3800 and 3500 cm^{-1} . Changes into spectra are related to the spectrum zone recognized to show vibrations from the crystalline domains.

4. Conclusions

It was verified that signals between 3800 and 3500 cm^{-1} are associated with hydroxyl groups of amylose and amylopectin. In addition, the main contribution to signals around 3300 cm^{-1} is associated with water molecules absorbed on the polymer matrix. Likewise, it was evidenced that the broadening and variations in the intensity of the maximum absorbance signals are related to neighboring hydroxyl groups. As a result of heating, starch

infrared spectrum experiment changes in the intensity of its signals. These changes permit one to define two zones in function of the use. The first one between 3800 and 2800 cm^{-1} related to the effect of thermal stress on intermolecular structure of starch, whereas the second one, under 2800 cm^{-1} , is useful for a structural description of starch. In particular, the FEDS technique in conjunction with DFT calculations have been demonstrated to be a useful tool for the high-precision spectral analysis of polymers subjected to small thermal perturbations, which would allow the implementation of spectral techniques instead of thermal ones for out-lab evaluations and for the study of thermal stress of biomaterials.

Author Contributions: V.G.: Data collection, analysis, interpretation, writing and review of the article. A.G.-Q.: Data collection, analysis, interpretation, writing and review of the article. T.A.L.: Data collection, analysis, interpretation, writing and review of the article. M.P.: Conceptualization, data collection, analysis, interpretation, writing and review of the article. E.M.C.: Data collection, analysis, interpretation, writing and review of the article. Á.A.A.: Data collection, analysis, interpretation, writing and review of the article. All authors have read and agreed to the published version of the manuscript.

Funding: This research was funded by the Sistema General de Regalias (SGR) through the Departamento Nacional de Planeación (DNP) of Colombia, Universidad del Valle, Universidad de Córdoba and Universidad de Sucre in the framework of the bicentennial calls, grant number BPIN 2020000100027.

Institutional Review Board Statement: Not applicable.

Informed Consent Statement: Not applicable.

Data Availability Statement: Data sharing not applicable.

Acknowledgments: Authors acknowledge to Universidad del Valle, Universidad de Córdoba, Universidad de Sucre and SGR-DNP of Colombia for the funds (Project with BPIN 2020000100027).

Conflicts of Interest: The authors declare no conflict of interest. The funders had no role in the design of the study; in the collection, analyses, or interpretation of data; in the writing of the manuscript; or in the decision to publish the results.

References

1. Teleky, B.E.; Dan, C.V. Biomass-derived production of itaconic acid as a building block in specialty polymers. *Polymers* **2019**, *11*, 1035. [[CrossRef](#)]
2. Pellis, A.; Malinconico, M.; Guarneri, A.; Gardossi, L. Renewable polymers and plastics: Performance beyond the green. *New Biotechnol.* **2021**, *60*, 146–158. [[CrossRef](#)]
3. Chi, H.; Xu, K.; Wu, X.; Chen, Q.; Xue, D.; Song, C.; Zhang, W.; Wang, P. Effect of Acetylation on the Properties of Corn Starch. *Food Chem.* **2008**, *106*, 923–928. [[CrossRef](#)]
4. Diop, C.I.K.; Li, H.L.; Xie, B.J.; Shi, J. Impact of the Catalytic Activity of Iodine on the Granule Morphology, Crystalline Structure, Thermal Properties and Water Solubility of Acetylated Corn (Zea Mays) Starch Synthesized under Microwave Assistance. *Ind. Crop. Prod.* **2011**, *33*, 302–309. [[CrossRef](#)]
5. Garces, V.; Palencia, M.; Combatt, E.M. Development of Bacterial Inoculums Based on Biodegradable Hydrogels for Agricultural Applications. *J. Sci. Technol. Appl.* **2017**, *2*, 13–23. [[CrossRef](#)]
6. Palencia, M.; Mora, M.; Palencia, S. Biodegradable Polymer Hydrogels Based in Sorbitol and Citric Acid for Controlled Release of Bioactive Substances from Plants (Polyphenols). *Curr. Chem. Biol.* **2017**, *11*, 36–43. [[CrossRef](#)]
7. Rodríguez-Pineda, L.M.; Muñoz-Prieto, E.D.J.; Rius-Alonso, C.A.; Palacios-Alquisira, J. Preparation and Characterization of Potato Starch Microparticles with Acrylamide by Microwave Radiation. *Cienc. Desarro.* **2018**, *9*, 149–159. [[CrossRef](#)]
8. Arrieta-Almario, A.A.; Mendoza-Fandiño, J.M.; Palencia-Luna, M.S. Composite Material Elaborated from Conducting Biopolymer Cassava Starch and Polyaniline. *Rev. Mex. Ing. Química* **2019**, *19*, 707–715. [[CrossRef](#)]
9. Palencia, M.; Lerma, T.; Garcés, V.; Mora, M.; Martínez, J.; Palencia, S.L. Principles of polymer synthetic green chemistry. In *Eco-Friendly Functional Polymers: An Approach from Application-Targeted Green Chemistry*, 1st ed.; Elsevier Science Publishing Co Inc: New York, NY, USA, 2021; pp. 5–22.
10. Arrieta, A.; Palencia, M. Estudio Electroquímico de Un Biopolímero Compuesto PPy/Almidón de Cassava. *Rev. Latinoam. Metal. Mater.* **2016**, *36*, 26–35.
11. Arrieta, A.; Combatt, E.; Palencia, M. Electrochemical Study of Cassava Starch Conductive Biopolymers Synthesized at Different PH. *Adv. J. Food Sci. Technol.* **2018**, *15*, 148–151. [[CrossRef](#)]

12. Wang, S.; Kong, L.; Zhao, Y.; Tan, L.; Zhang, J.; Du, Z.; Zhang, H. Lipophilization and Molecular Encapsulation of p-Coumaric Acid by Amylose Inclusion Complex. *Food Hydrocoll.* **2019**, *93*, 270–275. [[CrossRef](#)]
13. Maraphum, K.; Saengprachatanarug, K.; Wongpichet, S.; Phuphaphud, A.; Posom, J. In-Field Measurement of Starch Content of Cassava Tubers Using Handheld Vis-near Infrared Spectroscopy Implemented for Breeding Programmes. *Comput. Electron. Agric.* **2020**, *175*, 105607. [[CrossRef](#)]
14. Olagunju, A.I.; Omoba, O.S.; Enujiugha, V.N.; Wiens, R.A.; Gough, K.M.; Aluko, R.E. Influence of Acetylation on Physicochemical and Morphological Characteristics of Pigeon Pea Starch. *Food Hydrocoll.* **2020**, *100*, 105424. [[CrossRef](#)]
15. Omoregie, H. Chemical Properties of Starch and Its Application in the Food Industry. In *Chemical Properties of Starch*, 1st ed.; Emeje, M., Ed.; IntechOpen: London, UK, 2020. [[CrossRef](#)]
16. Schnupf, U.; Willett, J.L.; Bosma, W.; Momany, F.A. DFT Conformation and Energies of Amylose Fragments at Atomic Resolution. Part 1: Syn Forms of α -Maltotetraose. *Carboh. Res.* **2009**, *344*, 362–373. [[CrossRef](#)] [[PubMed](#)]
17. Afanasjeva, N.; Castillo, L.; Sinisterra, J. Biomasa Lignocelulósica. Parte I: Transformación de biomasa. *J. Sci. Technol. Appl.* **2017**, *3*, 27–43. [[CrossRef](#)]
18. Fu, H.Y.; Li, H.D.; Xu, L.; Yin, Q.B.; Yang, T.M.; Ni, C.; Cai, C.B.; Yang, J.; She, Y.B. Detection of Unexpected Frauds: Screening and Quantification of Maleic Acid in Cassava Starch by Fourier Transform Near-Infrared Spectroscopy. *Food Chem.* **2017**, *227*, 322–328. [[CrossRef](#)] [[PubMed](#)]
19. Paixão e Silva, G.D.L.; Bento, J.A.C.; Soares Júnior, M.S.; Caliari, M. Trend of Modification by Autoclave at Low Pressure and by Natural Fermentation in Sweet Potato and Cassava Starches. *Polysaccharides* **2021**, *2*, 354–372. [[CrossRef](#)]
20. Santha, N.; Sudha, K.G.; Vijayakumari, K.P.; Nayar, V.U.; Moorthy, S.N. Raman and Infrared Spectra of Starch Samples of Sweet Potato and Cassava. *J. Chem. Sci.* **1990**, *102*, 705–712. [[CrossRef](#)]
21. Warren, F.J.; Gidley, M.J.; Flanagan, B.M. Infrared Spectroscopy as a Tool to Characterise Starch Ordered Structure—a Joint FTIR–ATR, NMR, XRD and DSC Study. *Carb. Pol.* **2016**, *139*, 35–42. [[CrossRef](#)] [[PubMed](#)]
22. Garces, V.; Palencia, M. Biosynthesis and Biotransformations of Biopolymers: Starch and Poly(Hydroxyalkanoates). *J. Sci. Technol. Appl.* **2020**, *9*, 4–9. [[CrossRef](#)]
23. Pigłowska, M.; Kurc, B.; Rymaniak, Ł.; Lijewski, P.; Fuć, P. Kinetics and Thermodynamics of Thermal Degradation of Different Starches and Estimation the OH Group and H₂O Content on the Surface by TG/DTG-DTA. *Polymers* **2020**, *12*, 357. [[CrossRef](#)] [[PubMed](#)]
24. Paulik, S.; Jekle, M.; Becker, T. Mechanically and Thermally Induced Degradation and Modification of Cereal Biopolymers during Grinding. *Polymers* **2019**, *11*, 448. [[CrossRef](#)] [[PubMed](#)]
25. Kačíková, D.; Kubovský, I.; Ulbriková, N.; Kačík, F. The Impact of Thermal Treatment on Structural Changes of Teak and Iroko Wood Lignins. *Appl. Sci.* **2020**, *10*, 5021. [[CrossRef](#)]
26. Hashimoto, T.; Nakamura, Y.; Tamada, Y.; Kurosu, H.; Kameda, T. The influence of thermal treatments on the secondary structure of silk fibroin scaffolds and their interaction with fibroblasts. *PeerJ Mater. Sci.* **2020**, *2*, e8. [[CrossRef](#)]
27. Faroongsarn, D.; Wongpoowarak, W.; Mitrevej, A. Starch gelatinization under thermal stress. *Pharm. Dev. Technol.* **1999**, *4*, 531–538. [[CrossRef](#)]
28. Lu, D.L.; Yang, H.; Shen, X.; Lu, W.P. Effects of high temperature during grain filling on physicochemical properties of waxy maize starch. *J. Integrat. Agr.* **2016**, *15*, 309–316. [[CrossRef](#)]
29. Palencia, M.; Lerma, T.A.; Combatt, E.M. Hydrogels Based in Cassava Starch with Antibacterial Activity for Controlled Release of Cysteamine-Silver Nanostructured Agents. *Curr. Chem. Biol.* **2017**, *11*, 28–35. [[CrossRef](#)]
30. Palencia, M.; Lerma, T.; Garcés, V.; Mora, M.; Martínez, J.; Palencia, S.L. Polymer biosynthesis and biotransformations. In *Eco-Friendly Functional Polymers: An Approach from Application-Targeted Green Chemistry*, 1st ed.; Elsevier Science Publishing Co Inc: Cambridge, MA, USA, 2021; pp. 89–104.
31. Otálora, A.; Palencia, M. Application of Functionally-Enhanced Derivative Spectroscopy (FEDS) to the Problem of the Overlap of Spectral Signals in Binary Mixtures: Triethylamine-Acetone. *J. Sci. Technol. Appl.* **2019**, *6*, 96–107. [[CrossRef](#)]
32. Bantadjan, Y.; Rittiron, R.; Malithong, K.; Narongwongwattana, S. Establishment of an Accurate Starch Content Analysis System for Fresh Cassava Roots Using Short-Wavelength Near Infrared Spectroscopy. *ACS Omega* **2020**, *5*, 11210–11216. [[CrossRef](#)]
33. Ferreira-Villadiego, J.; Garcia-Echeverri, J.; Vidal Mejia, M.V.; Pasqualino, J.; Meza-Catellar, P.; Lambis, H. Chemical Modification and Characterization of Starch Derived from Plantain (*Musa Paradisiaca*) Peel Waste, as a Source of Biodegradable Material. *Chem. Eng. Trans.* **2018**, *65*, 763–768. [[CrossRef](#)]
34. Awolu, O.O.; Odoro, J.W.; Adeloye, J.B.; Lawal, O.M. Physicochemical Evaluation and Fourier Transform Infrared Spectroscopy Characterization of Quality Protein Maize Starch Subjected to Different Modifications. *J. Food Sci.* **2020**, *85*, 3052–3060. [[CrossRef](#)] [[PubMed](#)]
35. Palencia, M. Functionally-Enhanced Derivative Spectroscopy (FEDS): A Methodological Approach. *J. Sci. Technol. Appl.* **2020**, *9*, 29–34. [[CrossRef](#)]
36. Palencia, M. Functional transformation of Fourier-transform mid-infrared spectrum for improving spectral specificity by simple algorithm based on wavelet-like functions. *J. Adv. Res.* **2018**, *14*, 53–62. [[CrossRef](#)]
37. Restrepo, D.F.; Palencia, M.; Palencia, V.J. Study by Attenuated Total Reflectance Spectroscopy of Structural Changes of Humified Organic Matter by Chemical Perturbations via Alkaline Dissolution. *J. Sci. Technol. Appl.* **2018**, *4*, 49–59. [[CrossRef](#)]

38. García-Quintero, A.; Combatt, E.M.; Palencia, M. Structural Study of Humin and Its Interaction with Humic Acids by Fourier-Transform Mid-Infrared Spectroscopy. *J. Sci. Technol. Appl.* **2018**, *4*, 28–39. [[CrossRef](#)]
39. Lerma, T.A.; Garcés, V.; Palencia, M. Novel Multi- and Bio-Functional Hybrid Polymer Hydrogels Based on Bentonite-Poly(Acrylic Acid) Composites and Sorbitol Polyesters: Structural and Functional Characterization. *Eur. Polym. J.* **2020**, *128*, 109627. [[CrossRef](#)]
40. Palencia, S.L.; García, A.; Palencia, M. Mid-Infrared Vibrational Spectrum Characterization of the Outer Surface of *Candida Albicans* by Functionally Enhanced Derivative Spectroscopy. *J. Appl. Spectrosc.* **2021**, *88*, 166–180. [[CrossRef](#)]
41. Palencia, S.L.; García, A.; Palencia, M. Multiple Surface Interaction Mechanisms Direct the Anchoring, Co-Aggregation and Formation of Dual-Species Biofilm between *Candida Albicans* and *Helicobacter Pylori*. *J. Adv. Res.* **2021**. [[CrossRef](#)]
42. Anaya-Tatis, L.R.; Libreros, K.H.; Palencia, V.J.; Atencio, V.J.; Palencia, M. Mid-Infrared Spectral Characterization of Fish Scales: “Bocachico” (*Prochilodus Magdalenae*) by Functionally-Enhanced Derivative Spectroscopy (FEDS)—A Methodological Approach. *J. Sci. Technol. Appl.* **2019**, *6*, 28–39. [[CrossRef](#)]
43. Palencia, M. Deconvolution of IR Spectra by Functionally-Enhanced Derivative Spectroscopy (FEDS): Why Does It Work? *J. Sci. Technol. Appl.* **2020**, *9*, 18–28. [[CrossRef](#)]
44. Gao, X.; Liu, W.; Liu, H.; He, S.; Tang, M.; Zhu, C. Reaction Mechanism of Chitosan/Acrylamides Dimer: A DFT Study. *J. Phys. Org. Chem.* **2017**, *31*, e3775. [[CrossRef](#)]
45. Kazachenko, A.S.; Tomilin, F.N.; Pozdnyakova, A.A.; Vasilyeva, N. Yu.; Malyar, Y.N.; Kuznetsova, S.A.; Avramov, P.V. Theoretical DFT Interpretation of Infrared Spectra of Biologically Active Arabinogalactan Sulphated Derivatives. *Chem. Pap.* **2020**, *74*, 4103–4113. [[CrossRef](#)]
46. Nikonenko, N.A.; Buslov, D.K.; Sushiko, N.I.; Zhbakov, R.G. Investigation of Stretching Vibrations of Glycosidic Linkages in Disaccharides and Polysaccharides with Use of IR Spectra Deconvolution. *Biopolymers* **2000**, *57*, 257–262. [[CrossRef](#)]
47. Mina, J.; Valadez-González, A.; Herrera-Franco, P.; Zuluaga, F.; Delvasto, S. Physicochemical characterization of natural and acetylated thermoplastic cassava starch. *Dyna* **2011**, *78*, 166–173.
48. Lomeli, M.G.; Barrios-Guzman, A.J.; García, S.; Rivera-Prado, J.; Manríquez-González, R. Chemical and Mechanical Evaluation of Bio-composites Based on Thermoplastic Starch and Wood Particles Prepared by Thermal Compression. *Bioresources* **2014**, *9*, 2960–2974. [[CrossRef](#)]
49. Nybacka, L. FTIR Spectroscopy of Glucose. Degree of Bachelor, Master Programme in Electrical Engineering, Uppsala Universitet, Uppsala, Sweden, 2016.
50. Xie, F.; Zhang, B.; Wang, D.K. Starch Thermal Processing. In *Starch-Based Materials in Food Packaging*; Elsevier Inc.: Amsterdam, The Netherlands, 2017; pp. 187–227.
51. Morley, M.J.; Miles, C.A. Modelling the thermal conductivity of starch-water gels. *J. Food Eng.* **1997**, *33*, 1–14. [[CrossRef](#)]
52. Sopa, C.; Cumnueng, W.; Thavachai, T.; Juntanee, U.; Jatuphong, V. Effects of temperature and concentration on thermal properties of cassava starch solutions. *Songklanakarin J. Sci. Technol.* **2008**, *30*, 405–411.
53. Vahur, S.; Teearu, A.; Peets, P.; Joosu, L.; Leito, I. ATR-FT-IR spectral collection of conservation materials in the extended region of 4000–80 cm⁻¹. *Anal. Bioanal. Chem.* **2016**, *408*, 3373–3379. [[CrossRef](#)] [[PubMed](#)]
54. Ibrahim, M.; Alaam, M.; El-Haes, H.; Jalbout, A.F.; de Leon, A. Analysis of the structure and vibrational spectra of glucose and fructose. *Elect. Química* **2006**, *31*, 15–21. [[CrossRef](#)]